TELKOMNIKA, Vol.17, No.1, February 2019, pp.60~67
ISSN: 1693-6930, accredited First Grade by Kemenristekdikti, Decree No: 21/E/KPT/2018
DOI: 10.12928/TELKOMNIKA.v17i1.11598

Dual-band aperture coupled antenna with harmonic suppression capability

Faza Syahirah Mohd Noor*[1], Zahriladha Zakaria[2], Herwansyah Lago[3], Maizatul Alice Meor Said[4]
Centre of Telecommunication Research and Innovation (CeTRI),
Faculty of Electronics and Computer Engineering, Universiti Teknikal Malaysia Melaka (UTeM),
Hang Tuah Jaya, 76100, Durian Tunggal, Melaka, Malaysia
*Corresponding author, e-mail: fazasyahirah02@gmail.com[1], zahriladha@utem.edu.my[2],
herwansyahlago@gmail.com[3], maizatul@utem.edu.my[4]

Abstract

The paper presents an aperture-coupled dual-band linearly-polarized antenna with harmonic suppression capability, operating at frequency 2.45 GHz and 5.00 GHz. In purpose of improving the directivity of antenna at the operating frequency of 2.45 GHz and 5.00 GHz, a modified inverted π-shaped slot-etched patch on the lower layer of the stacked antenna is introduced alongside the 50 Ω feed line. The harmonic suppression capability is achieved by the introduction of U-slot and asymmetrical left-right-handed stub at the transmission feed line, suppressing unwanted harmonic signals from 6.00 GHz up to 10.00 GHz. The final design of the antenna has produced very good reflection coefficient of -18.87 dB at 2.45 GHz and -19.57 dB at 5.00 GHz with third and higher order harmonic suppression up to -4 dB.

Keywords*: asymmetrical left-right-handed stub, dual-band, harmonic suppression, u-slot*

1. Introduction

The rapid development in telecommunication particularly in the territory of wireless application has made gigantic requests for high performance antenna keeping in mind the end goal to fulfill superior ability without tempering the ecological difficulties to the completion. As indicated by the frequency spectrum as issued by the Malaysian Communications and Multimedia Commissions (MCMC) on December 2014, the point to multipoint spectrum for Wireless Local Area Network (WLAN) comprises of three resounding frequencies; 2.45 GHz (2400–2500 MHz), 5.25 GHz (5125–5325 MHz), and 5.8 GHz (5725–5875 MHz) [1]. The dual-band frequency operating at 2.45 GHz and 5.00 GHz are chosen as it is the commonly used band in the modern Wi-Fi router or access points such as from the router Cisco Aironet 3700 series for indoor and Cisco Aironet 1520 series for outdoor deployment [2].

In radio frequency (RF) applications, there are existence of ambient RF signals that can be harvested or also commonly known as energy harvesting [3]. Electromagnetic interference (EMI) resulting from active integrated microstrip antenna systems is not something new in RF technology. The non-linearity characteristics of active components as illustrated in RF energy harvesting block diagrams contributes to the creation of harmonics [4, 5]. In order to suppress or minimize the unwanted harmonic signals at higher order, it is crucial to implement the harmonic suppression filter into the system to avoid EMI radiation which easily produced by the non-linear circuit component of the system [6]. Unfortunately, the filtering technique may lead to the increment of the antenna size and disturbance to the matching network of the antenna and power loss at high frequencies [7]. Regardless the limitations due to the active components, there are many other techniques can be implemented to solve this problem [8] such as from the modification vias and stub loaded on the patch element [9], slot and symmetrical arm of stub at the transmission feed line [10], and stub-loaded resonators [11]. The past researcher in [12] also emphasize on the effect of the input impedance which at twice the desired frequency, the input impedance should be near to zero for the second harmonic not to be produced, and this is also been implemented in [13] with the quarter-wave section at the transmission feed line. Apart from technique implemented, there are various types of antenna structures that possess the

Received May 31, 2018; Revised November 8, 2018; Accepted December 7, 2018

energy harvesting capability such as stacked antenna [14], dipole antenna [15], microstrip patch antenna [16], and dual-rhombic loop antenna [17]. Different design structures of these antennas are suited to be used for different applications however the ability of energy harvesting is only limited to single frequency ambient signal.

For the past few years, researchers have focus on the antenna design which possess the integrated harmonic suppression capability within an antenna. According to the findings by [18], the antenna overall physical size is reduced using the fractal design and with the introductory of H-shaped defected ground structure (DGS) to suppress the harmonics created from the fractal iteration, thus the complexity of the antenna geometry increased. The implementation of defected ground structure (DGS) in [19] caused the patch size to be reduced to 26.7x30 mm^2, together with notch-loaded and curvature slots being introduced to suppress higher-order harmonics.

Different techniques implemented such as in [20-25], introduced the reflection coefficient of less than -3 dB of higher order harmonics, however the application of the antenna is limited to the functionality of single-band frequency application. The vision of green technology can be seen to be implied where most of the design are much more compact with the same structural physical antenna have been achieved in order to reduce development cost and sustain the environment. The comparison of past research study and the proposed antenna are tabulated in Table 1.

Table 1. Comparison of the Proposed Antenna and Past Research Work

Ref.	Technique	Performance
[18]	Defected ground structure	Suppress higher harmonic, out of band generated by first, second and third fractal iterations
[20]	Spur-line	Suppression up to -3 dB reflection coefficient
[21]	U-slot and symmetrical arm of inverted U-stub on microstrip feed line	Suppression up to -0.51 dB and -2.28 dB reflection coefficient at second and third harmonics
[22]	Aperture coupling slot with right-angled triangle shape	Band rejection capability ranging from 3 GHz up to 10 GHz
[23]	Radial stub on microstrip patch	Reflection coefficient of -1.92 dB at second harmonic
[24]	Partial ring defected ground structure with single open-ended stub	Band rejection of harmonic signals from 6 GHz up to 12 GHz
[25]	Unbalanced slots and dumbbell shape defected ground structure (DGS)	Rejection of second and third harmonic up to -2 dB reflection coefficient
Proposed	U-slot and asymmetrical stub embedded at the feed line	Dual-band characteristics with harmonic signals suppressed from frequency range of 6.00 GHz to 10.00 GHz

Based upon authors literature review and knowledge findings, the study by previous researchers focused more on either single-band frequency characteristic or, multi-band frequency of that 0.9 GHz and 2.45 GHz and very small amount of study which involved multi-band frequency response of that WLAN frequency spectrum. For this paper, a dual-band aperture coupled antenna at frequency 2.45 GHz and 5.00 GHz with the ability of harmonic suppression of the third and higher order is presented. In addition, the proposed design demonstrated the significant findings of asymmetrical stub on the frequency harmonics, achieving dual-band frequency response without having to have temper down significantly the reflection coefficient response of the second harmonic.

2. Antenna Design

For this project, the antenna is required to be functioning for the WLAN application thus, the resonant frequency of 2.45 GHz and 5.00 GHz are chosen. As for the board, FR4 substrate is chosen and has the dielectric constant, ε_r 4.4, loss tangent 0.019, dielectric height, h of

1.6 mm and double sided copper conductor with height, t of 0.035 mm. The dimensions of the antenna can be determined using the formula given in [18], [25].

$$Width\ of\ patch,\ \mathrm{W} = \frac{\mathrm{c}}{2\,\mathrm{f}_o}\sqrt{\frac{2}{\varepsilon \mathrm{r}+1}} \quad (1)$$

$$\text{Effective permittivty, } \varepsilon_{eff} = \frac{\varepsilon_r+1}{2} + \frac{\varepsilon_r-1}{2}\left[1+12\frac{\mathrm{h}}{\mathrm{w}}\right]^{-\frac{1}{2}} \quad (2)$$

$$\text{Effective length, } \mathrm{L}_{eff} = \frac{\mathrm{c}}{2\,\mathrm{f}_o\sqrt{\varepsilon\ \mathrm{eff}}} \quad (3)$$

$$\Delta \mathrm{L} = 0.412(\mathrm{h})\frac{(\varepsilon\ \mathrm{eff}+0.3)\left(\frac{\mathrm{w}}{\mathrm{h}}+0.264\right)}{(\varepsilon\ \mathrm{eff}-0.258)\left(\frac{\mathrm{w}}{\mathrm{h}}+0.8\right)} \quad (4)$$

$$\text{Length of patch, } \mathrm{L} = \mathrm{L}_{eff} - 2\Delta L \quad (5)$$

where;

f_o = resonant frequency
c = speed of light; $3x10^8$ ms^{-1}
ε_r = dielectric constant of substrate
ε_{eff} = effective dielectric constant of patch
h = substrate thickness

2.1. Antenna Geometry

Figure 1 shows the geometry and dimension of the proposed inverted π-shaped slot-etched aperture coupled antenna with the capability of dual-band operation, at which it is being excited with 50 Ω microstrip feed line. Figure 2 shows the proposed antenna design with the dimension of 80 mmx80 mmx5.07 mm. The detailed antenna dimensions are illustrated as in Figures 1 (a)-(e).

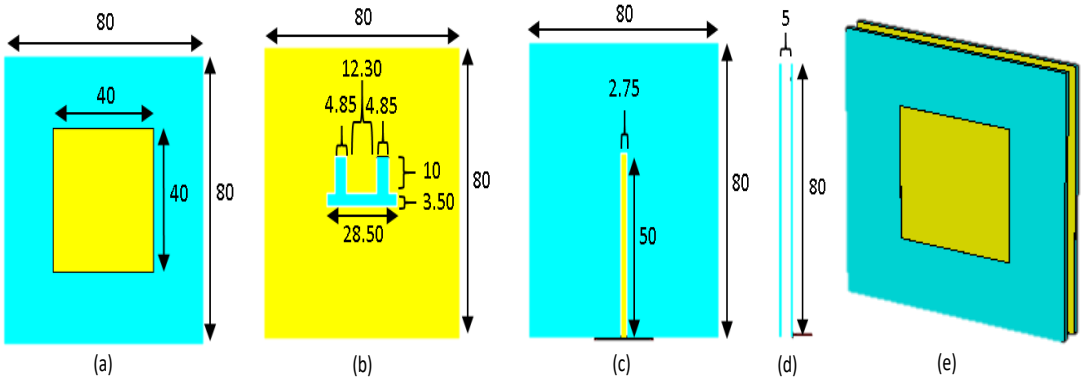

Figure 1. Antenna layout with design specifications using CST software;
(a) top view (upper layer substrate), (b) top view (lower layer substrate),
(c) bottom view (lower layer substrate), (d) side view, and (e) perspective view

2.2. U-slot and L-stub at the Feed line

Figure 2 illustrates the initial geometry and dimension of the transmission feed line of inverted π-shaped slot-etched aperture-coupled antenna with the capability of multi-band operation where it is also being excited using 50 Ω microstrip feed line. Figure 3 shows the proposed feed line design with the harmonic suppression technique as implemented in [16], [21]. The proposed harmonic suppression technique are illustrated as in Figure 3 (a)-(d).

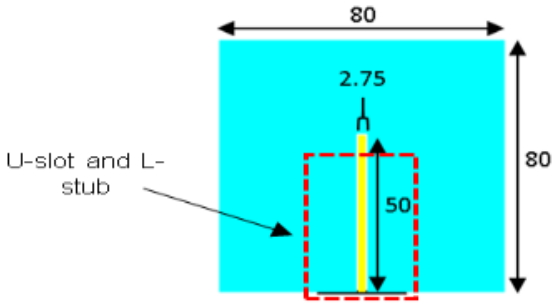

Figure 2. Initial transmission feed line

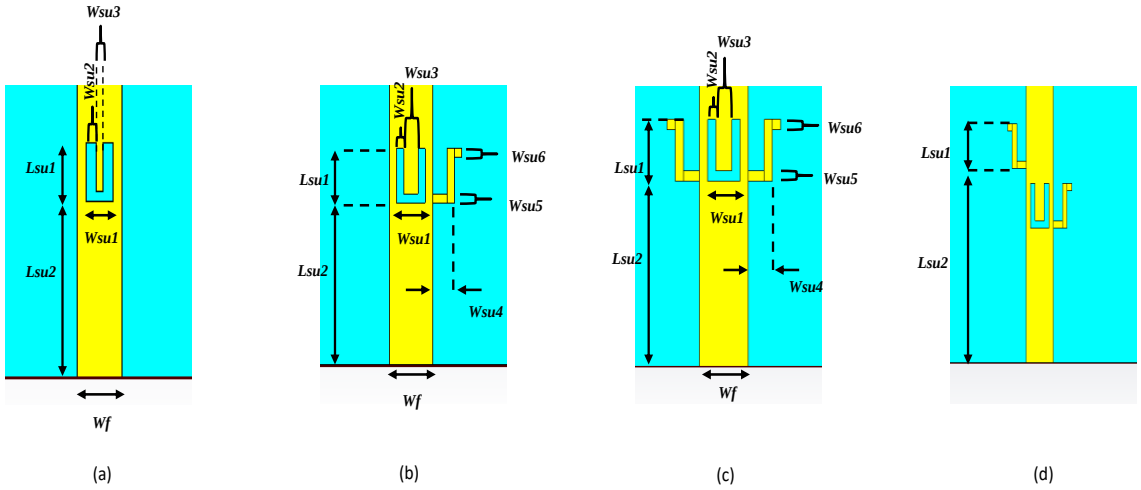

Figure 3. Transmission feed line; (a) Embedded U-slot, (b) Combination of U-slot and right-handed stub, (c) Combination of U-slot and symmetrical stub, (d) Combination of U-slot and asymmetrical stub

3. Results and Analysis

The reflection coefficient parameter of different transmission feed line topology as illustrated as in Figure 2 and Figures 3 (a)-(d) are highlighted in Figure 4. The graphical illustration highlights the differences on the resonant frequency and the reflection coefficient responses. Based on the observation, the initial design of the transmission line as illustrated in Figure 2, produces three resonant frequencies of 2.45 GHz, 5.00 GHz and 9 GHz with reflection coefficient of -30.096 dB, -21.143 dB, and -26.253 dB respectively. The proposed embedded U-slot at the feed line is observed to suppress the reflection coefficient at frequency 5.00 GHz, initially from -21.143 dB to -14.537 dB however with the proposed design, the fourth harmonic is being introduced at 9.45 GHz with the reflection coefficient of -43.439 dB. Since the introductory of U-slot is not sufficient to suppress the harmonics of higher than 5.00 GHz, stub is introduced to the feed line. The combination of U-slot and right-handed stub at the feed line is observed to suppress the higher harmonics of 5.00 GHz, while enhancing the reflection coefficient of the first two harmonics at 2.45 GHz and 5.00 GHz, producing reflection coefficient of -25.953 dB and -25.414 dB respectively. This design still produces third harmonic with reflection coefficient of smaller than -5 dB. Hence, the U-slot with symmetrical left-right-handed stub is analyzed and the reflection coefficient at 2.45 GHz is -18.889 dB and at 5.00 GHz is -19.416 dB. The proposed symmetrical stub is observed to enhance the frequency response of the second resonant frequency however, also enhancing the reflection coefficient at 7.3 GHz from -4.886 dB to -8.587 dB. The current distribution of the feed line is analyzed and from the concentrated electrical length, the feed line with U-slot and asymmetrical left-right-handed stub is proposed.

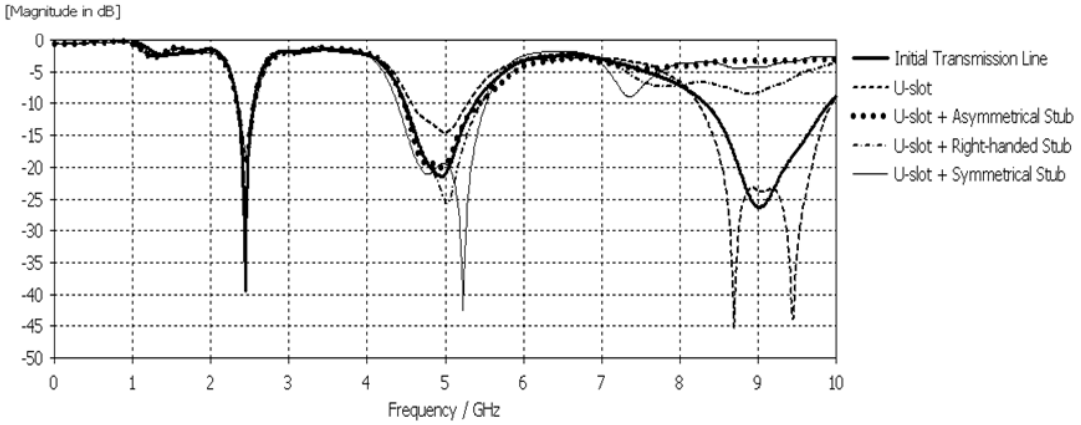

Figure 4. The comparison of simulation results on parameter reflection coefficient for different designs of transmission feed line

Figure 5 illustrates the reflection coefficient of antenna with the feed line design as illustrated in Figure 3 (d). The graphical illustration highlights the differences on the resonant frequencies and the reflection coefficient response. Based on the observation, the proposed U-slot and asymmetrical stub as illustrated in Figure 3 (d), produces two resonant frequencies of 2.45 GHz and 5.00 GHz with reflection coefficient of -18.872 dB and -19.566 dB respectively. The proposed design is observed to suppress the higher order harmonics generated at 7.3 GHz, 8.69 GHz, 9.00 GHz and 9.45 GHz. The outcome from the asymmetrical stub design has suppressed the unwanted third and higher order harmonics of reflection coefficient greater than -5 dB, ranging from the 6.00 GHz up to 10.00 GHz.The proposed asymmetrical stub design has produced dual-band resonant frequencies of almost similar reflection coefficient response at 2.45 GHz and 5.00 GHz whilst suppressing the third and higher order harmonics unlike the design proposed in [18-20], at which only focused on the operation single band frequency.

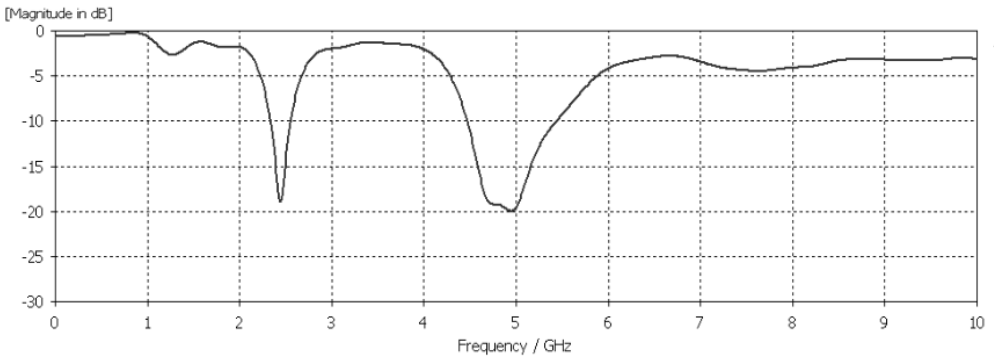

Figure 5. The simulation result on parameter reflection coefficient for the design of U-slot and asymmetrical left-right-handed stub

Figure 6 highlights the current distribution at transmission line, where the intensity of the current that flows into the main radiating elements of the antenna are further analyzed. Based on Figure 6 (a) and 6 (b), the intensity of the current distribution is larger than the intensity of that distribution at 7.3 GHz and 9 GHz. Figure 6 (c) and 6 (d) show that the current distribution is blocked from flowing into the main radiating slot at frequency 7.3 GHz and 9 GHz with the addition of U-slot and asymmetrical left-right-handed stub, completely suppressing the third and fourth harmonics response. These findings are also found in [26] which had revealed that the amount of current distributes into conductive element can be affected by the surface wave acting on it.

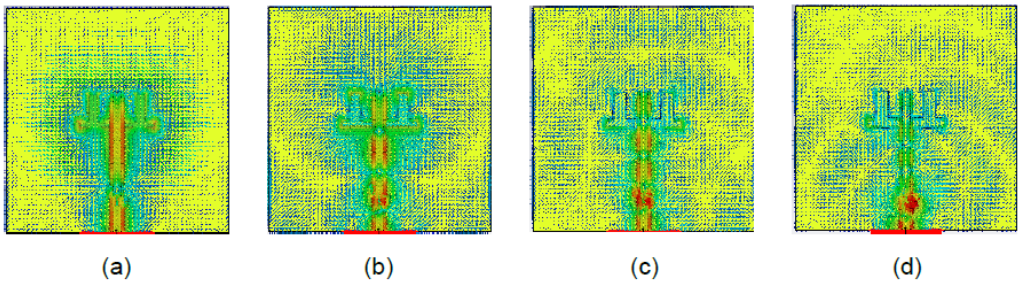

Figure 6. Current distribution at feed line:
(a) at 2.45 GHz, (b) at 5.00 GHz, (c) at 7.3 GHz, (d) at 9.00 GHz

3.1. Parametric Analysis on Parameter Lsu2

Optimization of the antenna structure is crucial in order to obtain better outcomes in terms of reflection coefficient, bandwidth and even the directivity of antenna. This optimization process can be done by conducting the parametric analysis on certain parameter of the antenna, and for this project mainly focusing on the position of stub towards the frequency response and reflection coefficient.

Figure 7 is the outcomes of the parametric analysis on position of stub, Lsu2. Based on the graph in Figure 7, there is slightly frequency shifting can be observed for both frequency bands but much more visible on the second frequency band, where the resonant frequency seems to be shifting more to higher frequency as the length increases by the increment of 1 mm. For this parameter, the value Lsu2=13 mm is chosen as the optimized value. The effect of the position of stub Lsu2 can be observed on the suppression of the third harmonic where the reflection coefficient is greater than -5 dB starting from 6.00 GHz to 10.00 GHz when Lsu2 is 13 mm. The value of Lsu2 at 14 mm is not the optimum value although the frequency response is almost similar to when it is 13 mm, and this is because when the Lsu2 is 14 mm, the reflection coefficient at 10.00 GHz can be observed to be greater than -5 dB and might as well produce the third harmonic at frequency of higher than 10.00 GHz. The reflection coefficient of the antenna from varying the parameter Lsu2 are tabulated in Table 2.

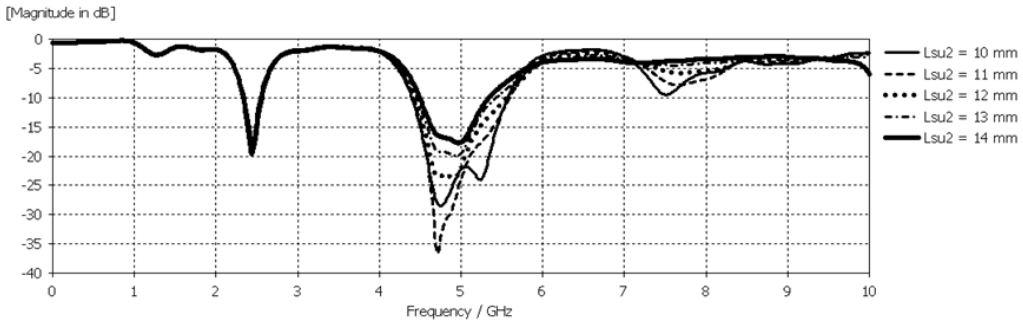

Figure 7. Parametric analysis on the effect position of stub, Lsu2 towards the antenna reflection coefficient

Table 2. Parametric Studies on Lsu2 of Asymmetrical Left-right-handed Stub

Lsu2 (mm)	Resonant frequency (GHz)		Reflection coefficient (dB)	
	Lower	Upper	Lower	Upper
9.00	2.46	5.23	-19.39	-42.41
10.00	2.46	4.75	-18.81	-28.49
11.00	2.45	4.71	-18.56	-36.67
12.00	2.44	4.92	-18.58	-23.61
13.00	2.45	5.00	-18.87	-19.57
14.00	2.45	5.00	-19.23	-17.63

4. Conclusion

A dual-band antenna as proposed in this paper has been designed and the desired resonant frequencies that applicable for WLAN application are achieved. The antenna design focuses on the effect of the slot and stub towards the current distribution at the transmission feed line for the purpose of harmonic suppression. The introduction of U-slot at the transmission feed line is for suppressing the third harmonic at frequency 9.00 GHz instead, another harmonic is generated at 8.69 GHz and the reflection coefficient response at 5.00 GHz also deteriorates from -21.143 dB to -14.537 dB. Together with the slot, a right-handed stub is introduced and the third and fourth harmonics are observed to be suppressed up to the reflection coefficient greater than -10 dB, however that value still allows current eventhough in small amount, to flow into the main radiating elements. In the same manner, left-right-handed stub design is further analyzed in comparison of symmetrical and asymmetrical structure of the stub on the antenna reflection coefficient, comparatively suppressing the third and higher order harmonics with the asymmetrical stub design. In essence, the asymmetrical stub design diverts the current distribution towards the stub instead of propagating into the main radiator patch thus creates more harmonic. The proposed U-slot with asymmetrical left-right-handed stub showed that harmonic suppression of third and higher order can be suppressed without having the first and second harmonics to be affected by it, where the reflection coefficient at 2.45 GHz and 5.00 GHz is -18.87 dB and -19.57 dB respectively, meanwhile at 7.3 GHz is less than -5 dB. The harmonic suppression is ranging from frequency 6.00 GHz up to 10.00 GHz and therefore is suitable for antenna with dual-band energy harvesting capability especially for the ambient RF energy harvesting from the WLAN applications.

Acknowledgments

The authors would like to express their thanks to the anonymous reviewers for their attentive reading of the research article, and for their constructive suggestions and feedbacks for the improvement of our work. The work was supported by UTeM under research grant PJP/2017/FKEKK/HI10/S01531.

References

[1] Malaysian Communications and Multimedia Commission. Guideline on The Provision of Wireless Local Area Network (WLAN) Service. Retrieved from https://www.mcmc.gov.my/skmmgovmy/media/General/pdf/Guideline_WirelessLAN.pdf , 2013.
[2] Cisco Aironet 3700 Series Access Points. Retrieved from https://www.cisco.com/c/en/us/products/collateral/wireless/3700-series-access-point/data_sheet_c78-729421.pdf, 2018.
[3] Veronique K, Cyril L, Fabrice S, Christian P. A Multi-Band Stacked RF Energy Harvester With RF-to-DC Efficiency Up to 84%. *IEEE Trans. Microwave Theory and Tech*. 2015; 63(5): 1768-1778.
[4] Khansalee E, Zhao Y, Leelarasmee E, Nuanyai K. A *Dual-Band Rectifier for RF Energy Harvesting Systems.* Electrical Engineering/Electronics, Computer, Telecommunications and Information Technology (ECTI-CON), 2014 11th International Conference. 2014. IEEE.
[5] Sun JS, Chen RH, Liu SK, Yang CF. Wireless Power Transmission with Circularly Polarized Rectenna. *Microwave Journal*. 2014; 1-15.
[6] X Yin, H Zhang, XY Huang, HY Xu. Spurious Modes Reduction in a Patch Antenna using an EBG-Based Microstrip Transmission Line Filter. *Progress in Electromagnetics Research C*. 2012; 25: 41-54.
[7] V Radisic, Y Qian, T Itoh. Novel Architectures for High-Efficiency Amplifiers for Wireless Applications. *IEEE Trans. Microwave Theory and Tech*. 1998; 46(11): 1901-1909.
[8] Nurzaimah Z, Zahriladha Z, Maisarah A, Mawarni MY. A Review of Antenna Designs with Harmonic Suppression for Wireless Power Transfer. *ARPN Journal of Engineering and Applied Sciences*. 2015; 10(11): 4842-4851.
[9] Xiao B, Wang X, Zhao J. A *Harmonic Suppression Microstrip Antenna for Mobile Communications Using Complementary Split Ring Resonators*. Proceedings of Annual Conference of China Institute of Communications. 2009; 491-493.
[10] Nurzaimah Z, Zahriladha Z, Maisarah A, Mawarni MY. Harmonic Suppression Rectangular Patch Antenna with Circularly Polarized. *TELKOMNIKA Telecommunication Computing Electronics and Control*. 2016; 14(2): 471-477.

[11] CX Mao, S Gao, Y. Wang, Q Luo, Q X Chu. A Shared-Aperture Dual-Band Dual-Polarized Filtering-Antenna-Array with Improved Frequency Response. *IEEE Transactions on Antennas and Propagation*. 2017; 65(4): 1836-1844.
[12] V Radisic, ST Chew, Y Qian, T. Itoh. High-Efficiency Power Amplifier Integrated with Antenna*. IEEE Microwave and Guided Wave Letters*. 1997; 7(2): 39-41.
[13] R.A. Rahim, S.I.S Hassan, F.Malek, M.N.Junita, H.F.Hassan. Harmonics Suppression Single-fed Dual-Circularly Polarized Microstrip Patch Antenna for Future Wireless Power Transmission. *International Journal of Engineering and Technology (IJET).* 2013; 5(5): 4423-4430.
[14] Nurzaimah Z, Zahriladha Z, Maisarah A, Mawarni MY. A 2.45 GHz Harmonic Suppression Rectangular Patch Antenna with Circular Polarization for Wireless Power Transfer Application. *IETE Journal of Research.* 2017; 64(3): 310-316.
[15] Berndie S, Kai C. 5.8-GHz Circularly Polarized Dual-Rhombic-Loop Traveling-Wave Rectifying Antenna for Low Power-Density Wireless Power Transmission Applications. *IEEE Trans. Microwave Theory and Tech*. 2003; 51(5): 1548-1553.
[16] Ugur O, Chi-Chih C, John LV. Investigation of Rectenna Array Configurations for Enhanced RF Power Harvesting. *IEEE Trans. Microwave Theory and Tech*. 2011; 10: 262-265.
[17] S.V. Kumar, P. Patel, A. Mittal. *Design, Analysis and Fabrication of Rectenna for Wireless Power Transmission–A Virtual Battery*. National Conference on Communication (NCC*). 2012*: 1-4.
[18] Prajapati PR. Application of Defected Ground Structure to Suppress Out-of-Band Harmonics for WLAN Microstrip Antenna. *International Journal of Microwave Science and Technology*. 2015; 1-9.
[19] R A Rahim, SIS Hassan, F Malek, M N Junita, M F Jamlos, M N Azizan. A 2.45 GHz *Harmonic Suppression Rectangular Patch Antenna.* 2012 International Symposium on Computer Applications and Industrial Electronics (ISCAIE 2012). 2012.
[20] Su G, Liao C, Zheng X, Wang S. *Harmonic Suppression with Spur-Line for Microstrip Patch Antenna*. 3rd IEEE International Symposium on Microwave, Antenna, Propagation and EMC Technologies for Wireless Communications. 2009. IEEE.
[21] Nurzaimah Z, Zahriladha Z, Maisarah A, Mawarni MY. A 2.45 GHz Harmonic Suppression Rectangular Patch Antenna with Circular Polarization for Wireless Power Transfer Application. *IETE Journal of Research*. 2017.
[22] S Ahmed, Z Zakaria, MN Husain, IM Ibrahim, A Alhegazi. Efficient feeding geometries for rectenna design at 2.45 GHz. *Electronics Letters*. 2017; 53(24): 1585-1587.
[23] Barrera OA, Lee DH, Quyet NM, Hoang-The V, Chang Parl H. A Circularly Polarized Harmonic-Rejecting Antenna for Wireless Power Transfer Applications. *IEICE Electronics Express*. 2013; 10(19):1-6.
[24] Biswas S, Guha D, Kumar C. Control of Higher Harmonics and Their Radiations In Microstrip Antennas Using Compact Defected Ground Structures. *IEEE Transactions on Antennas and Propagation*. 2013; 61(6): 3349-3353.
[25] Ong CS, Karim MF, Ong LC, Chiam TM, Aplhones A. A Compact 2x2 Circularly Polarized Antenna Array for Energy Harvesting. *Asia-Pacific Microwave Conference Proceedings (APMC).* 2010.
[26] Ningsih YK, Hadigenoro R. Low Mutual Coupling Dualband MIMO Microstrip Antenna Parasitic with Air Gap*. TELKOMNIKA Telecommunication Computing Electronics and Control.* 2014; 12(2): 405-410.